

Research Paper

Dissection of the Autophagosome Maturation Process by a Novel Reporter Protein, Tandem Fluorescent-Tagged LC3

Shunsuke Kimura¹

Takeshi Noda¹

Tamotsu Yoshimori^{1,2}

¹Research Institute for Microbial Diseases; Osaka University; Osaka, Japan

²CREST; Japan Science and Technology Agency; Kawaguchi-Saitama, Japan

*Correspondence to: Tamotsu Yoshimori; Research Institute for Microbial Diseases; Department of Cellular Regulation; 3-1 Yamadaoka; Suita, Osaka 565-0871 Japan; Tel.: +81.6.6879.8293; Fax: +81.06.6879.8295; Email: tamoyoshi@biken.osaka-u.ac.jp

Original manuscript submitted: 04/10/07

Manuscript accepted: 05/21/07

Previously published online as an *Autophagy* E-publication:

<http://www.landesbioscience.com/journals/autophagy/abstract.php?id=4451>

KEY WORDS

autophagosome, autolysosome, LC3, lysosome, GFP, mRFP, tandem fluorescent tag, pH, Rab7

ABBREVIATIONS

GFP	green fluorescent protein
mRFP	monomeric red fluorescent protein
CFP	cyan fluorescent protein
LC3	microtubule associated protein 1, light chain 3
tfLC3	tandem fluorescent tagged LC3
TMR	tetramethyl-rhodamine
TfR	transferrin receptor
MDC	monodansylcadaverine
Lamp1	lysosome-associated membrane protein 1

ACKNOWLEDGEMENTS

See page e8.

NOTE

Supplemental Material can be found at: www.landesbioscience.com/supplement/kimuraAUTO3-5-sup.pdf

ABSTRACT

During the process of autophagy, autophagosomes undergo a maturation process consisting of multiple fusions with endosomes and lysosomes, which provide an acidic environment and digestive function to the interior of the autophagosome. Here we found that a fusion protein of monomeric red-fluorescence protein and LC3, the most widely used marker for autophagosomes, exhibits a quite different localization pattern from that of GFP-LC3. GFP-LC3 loses fluorescence due to lysosomal acidic and degradative conditions but mRFP-LC3 does not, indicating that the latter can label the autophagic compartments both before and after fusion with lysosomes. Taking advantage of this property, we devised a novel method for dissecting the maturation process of autophagosomes. mRFP-GFP tandem fluorescent-tagged LC3 (tfLC3) showed a GFP and mRFP signal before the fusion with lysosomes, and exhibited only the mRFP signal subsequently. Using this method, we provided evidence that overexpression of a dominant negative form of Rab7 prevented the fusion of autophagosomes with lysosomes, suggesting that Rab7 is involved in this step. This method will be of general utility for analysis of the autophagosome maturation process.

INTRODUCTION

Autophagy is an intracellular bulk degradation system in which cytoplasmic components, such as proteins or organelles, are directed to the lysosome by a membrane-mediated process.^{1,2} In mammalian cells, this system is regulated by nutrient availability and hormones, and has been suggested to be essential for cellular homeostasis. In addition to its homeostatic function, autophagy plays quite important physiological roles such as in intracellular protein quality control under normal conditions,^{3,4} and as a defense mechanism against bacterial pathogens^{5,6} or the toxic effects of aggregate-prone proteins.^{7,8}

A small, flattened membrane sac structure, called the isolation membrane, elongates to surround a portion of the cytoplasm, and eventually forms a double-membrane structure, the autophagosome. Autophagosomes then undergo a maturation process consisting of multiple fusion events with both endosomes and lysosomes.^{2,9} Upon acquisition of lysosomal proteases and the vacuolar-type proton ATPase, the interior of the autophagosome becomes acidified, and cytoplasmic materials are subjected to degradation. Autophagosomes at this final stage, after fusion with lysosomes, are called autolysosomes.

Recent studies have shown that some molecules involved in the endocytic pathway also participate in autophagosome maturation in mammalian cells, such as Rab7, SKD1, Vti1b and presenilin 1.¹⁰⁻¹⁴ The fusion event of autophagosomes with endosomes and lysosomes has been mainly studied by morphological analysis using electron microscopy.⁹ In general, electron microscopy is not a particularly easy methodology because of the requirement for expensive equipment and skilled technical expertise. In addition, it is sometimes difficult to distinguish each maturation step of autophagosome biogenesis just by morphology. For example, the occurrence of each fusion event is not so evident just by ultrastructural analysis because lysosomes are sometimes much smaller than autophagosomes.

For the purpose of tracing the autophagic process, LC3 (microtubule-associated protein 1 (MAP1) light chain 3) is widely used as a marker protein. LC3, a mammalian homologue of yeast Atg8, undergoes post-translational modification by an ubiquitination-like reaction.¹⁵ The carboxyl terminal region of nascent LC3 (proLC3) is cleaved off to become a soluble form, LC3-I, exposing its carboxyl terminal glycine. At the glycine residue, LC3-I is modified with phosphatidylethanolamine and becomes a membrane-bound form, LC3-II; this step involves an ubiquitination-like reaction mediated by Atg7 (E1) and Atg3 (E2).¹⁶ The lipidated LC3-II is bound to both the outer and inner membrane

of the autophagosome. The formation of LC3-II is therefore a good marker to monitor the occurrence of autophagosome formation.¹⁵ LC3 localization is easily examined by observing chimeric proteins fused with green fluorescent protein (GFP), GFP-LC3 and the latter is widely used for an autophagosome marker.¹⁷

Here we found that GFP-LC3 and mRFP-LC3 show different localization patterns due to the different sensitivity of these fluorescent proteins to the lysosomal environment. GFP fluorescence was attenuated by acidic conditions and degraded by lysosomal hydrolases, whereas mRFP fluorescence was relatively stable. We utilized this finding to develop a novel marker protein, mRFP-GFP-LC3, for assessing the fusion step of autophagosomes with lysosomes. Autophagosomes marked by this marker protein showed both mRFP and GFP signals. After fusion with lysosomes, GFP signals were attenuated, and only mRFP signals were observed. Using this protein, we were able to prove that Rab7 is involved in the fusion step of autophagosomes with lysosomes.

MATERIALS AND METHODS

Cell culture and transfection. All cell lines were cultured in Dulbecco's modified Eagle's medium (Sigma) supplemented with 8% heat-inactivated fetal bovine serum (Gibco). Transfection was performed using LipofectAMINE2000 (Invitrogen) according to the manufacturer's protocol. For amino acid starvation, cells were cultured in Hanks' solution containing 10 mM HEPES (pH 7.5) without amino acids and fetal bovine serum for 2 hours. Stable transformants were selected in complete medium containing 500 µg/ml G418 (Sigma). Atg5-deficient mouse embryonic fibroblasts were described previously.¹⁸

Antibodies. Mouse monoclonal anti-Lamp1 (H4A3) (Santa Cruz), anti-HA (16B12) (Babco), anti-TfR (BD bioscience), goat anti-Aldolase (RockLand), rabbit anti-GFP and RFP antibody (MBL) are all commercially available. Anti-LC3 antibody against recombinant full length LC3 (SK2-6) was described previously.¹⁵

Plasmid construction. The plasmids pEGFP-LC3 and pEGFP-LC3 G120A were previously described.¹⁵ The plasmid pEGFP-C1 was purchased from Clontech. Rab7 cDNA was cloned from genomic DNA of MDCK cells, and inserted into pEGFP-C1 using exogenously added *Hind*III and *Xho*I sites, and a point mutation (T22N) was introduced by the KOD-Plus-Mutagenesis kit (Toyobo).

The plasmid encoding monomeric red fluorescent protein (mRFP) was a generous gift from Dr. Roger Y. Tsien (University of California, San Diego).¹⁹ For construction of the mRFP-LC3 plasmid, the PCR was used to generate mRFP cDNA with exogenous restriction sites of *Nhe*I and *Bgl*II at its 5' and 3' ends, respectively, and lacking the

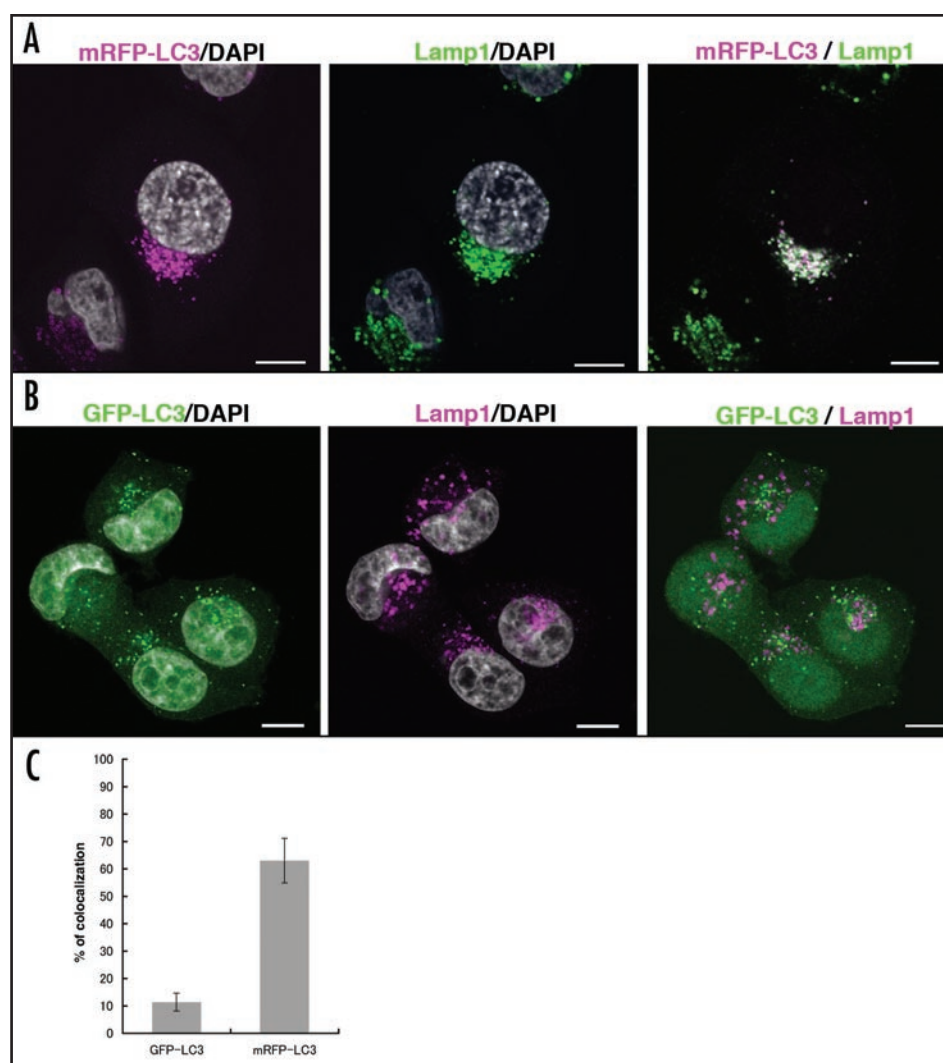


Figure 1. mRFP-LC3, but not GFP-LC3, colocalized with Lamp1. HeLa cells stably expressing mRFP-LC3 (A) or GFP-LC3 (B) were subjected to starvation in Hanks' solution for 2 hours and then fixed. Fixed cells were incubated with anti-Lamp1 monoclonal antibody and subsequently anti-mouse antibody conjugated to Alexa488 (A) or Alexa568 (B). Cells were observed with confocal microscopy. Nuclear staining was performed with DAPI (shown in grey in each panel). Bar indicates 10 µm. (C) Colocalization efficiency of mRFP- or GFP-LC3 puncta with Lamp1 was measured using ImageJ software, and shown as the percentage of the total number of mRFP- or GFP-LC3 puncta, respectively. The value indicates the average and S.D. from at least five images.

termination codon. The PCR fragment after digestion by each restriction enzyme was used to replace the EGFP cDNA of pEGFP-C1, and the resulting plasmid was named mRFP-C1. The *Bgl*II-*Eco*RI fragment of LC3 and the LC3 G120A mutant was inserted into the corresponding sites in the mRFP-C1 plasmid. For construction of the mRFP-GFP-LC3 plasmid, the PCR was used to generate mRFP cDNA with exogenously added *Nhe*I and *Age*I restriction sites at its 5' end and 3' ends, respectively, and lacking the termination codon using the following primers: *Nhe*I_mRFP (5'-GAGAGCTAGCGG CCACCATGGCCTCCTCCGAGGAC-3') and *Age*I_mRFP (5'-G AGAACCGGTCCACCGGCGCCGGTGGAGTGGCG-3'). The PCR product was digested by each restriction enzyme, and inserted into the *Nhe*I-*Age*I site of pEGFP-LC3 or pEGFP-LC3 G120A.

Immunocytochemistry and fluorescence microscopy. For immunofluorescence microscopy, cells were plated on 12 mm noncoated cover slips and then cultured for 24 hours. These cells were transferred

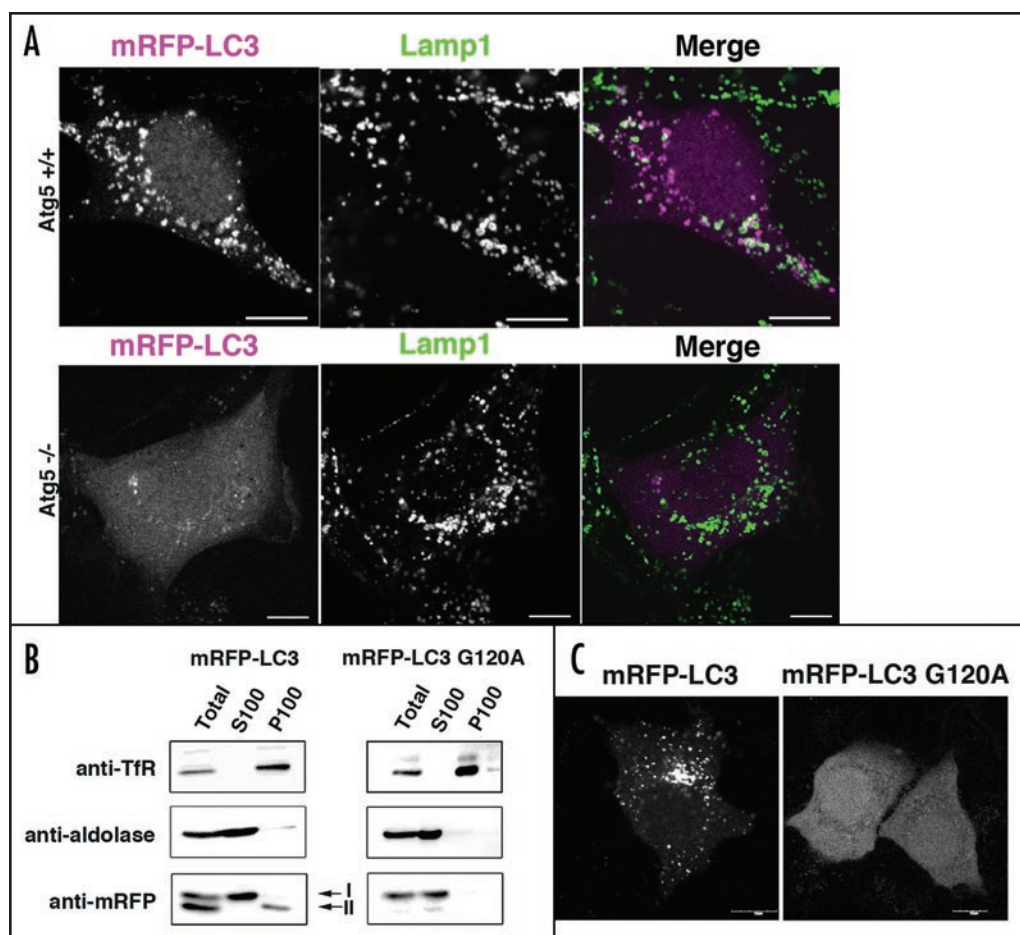


Figure 2. Lysosomal localization of mRFP-LC3 was dependent on Atg5 and C-terminal lipidation. (A) A plasmid expressing mRFP-LC3 was transfected into wild-type (upper panel) or Atg5-deficient (lower panel) mouse embryonic fibroblasts. Twenty-four hours after the transfection, the cells were subjected to starvation in Hanks' solution for 2 hours. After fixation the cells were subjected to immunocytochemistry using anti-Lamp1 antibody as described in Figure 1. (B) HeLa cells were transfected with a plasmid expressing mRFP-LC3 or mutant mRFP-LC3^{G120A}. Twenty-four hours after the transfection, the cells were subjected to starvation in Hanks' solution for 2 hours and then subjected to cell fractionation analysis. Cell lysate prepared as described in Materials and Methods was subjected to centrifugation at 10,000 \times g for 1 hour. Equivalent volumes of samples were resolved by SDS-PAGE and subjected to immunoblotting with each antibody. Total, S100 and P100 correspond to the total cell lysate, and the supernatant and pellet fractions, respectively, from 100,000 \times g centrifugation. TfR is transferrin receptor used as a membrane fraction marker. Aldolase was used as a soluble fraction marker. In the panel of mRFP, I and II correspond to mRFP-LC3-I and mRFP-LC3-II forms, respectively. (C) HeLa cells were transfected with a plasmid encoding mRFP-LC3 or mutant mRFP-LC3^{G120A}. Twenty-four hours after the transfection, the cells were subjected to starvation in Hanks' solution for two hours, then fixed and subjected to microscopy analysis.

to Hanks' medium, cultured for two hours, and then fixed with 3% paraformaldehyde in PBS at room temperature. After fixation, the cells were permeabilized with 50 μ g/ml digitonin in PBS for 5 min at room temperature. The cells were incubated with an anti-Lamp1 antibody (1:100 dilution) or anti-HA antibody (1:5000) for 1 hour at room temperature. After the second antibody treatment, samples were examined under a fluorescence laser scanning confocal microscope, FV1000 (Olympus).

Cell fractionation. HeLa cells transfected with the plasmid encoding mRFP-LC3, mRFP or the LC3 G120A mutant were washed, harvested in PBS containing protease inhibitor cocktail (Roche) and 1 mM phenylmethylsulfonyl fluoride, and homogenized with a sonicator four times for 5 sec each. After 1,000 \times g centrifugation of the homogenate, the supernatant (total fraction) was ultracentrifuged

for 60 min at 100,000 \times g (TLA-55 rotor; Beckman) at 4°C. After taking the supernatant as the soluble fraction, the pellet was sonicated and ultracentrifuged once more using the same conditions. The second supernatant was discarded and the resulting pellet (membrane fraction) and the supernatant (soluble fraction) from the first ultracentrifugation were resuspended in the homogenization buffer. Each fraction was diluted to equivalent volumes, and subjected to immunoblotting.

Immunoblotting. SDS-PAGE and immunoblotting was done as previously described.⁸ Each antibody was diluted as follows for immunoblotting: anti-transferrin receptor (TfR) monoclonal antibody (1:1000 dilution), anti-aldolase antibody (1:5000 dilution), anti-mRFP antibody (1:1000 dilution), anti-GFP antibody (1:1000 dilution), and anti-LC3 antibody (1:2000 dilution).

Protease inhibitors and ionophore treatment. E64d and pepstatin A, and nigericin were purchased from the Peptide Institute (Osaka, Japan) and Sigma, respectively. Tetramethyl-Rhodamine Dextran was purchased from Molecular Probes. HeLa cells stably expressing GFP-LC3 were cultured on non-coated glass-bottom culture dishes and incubated with 0.5 mg/ml of Tetramethyl-Rhodamine (TMR) Dextran over night for marking lysosomes. The cells were transferred to new culture medium and incubated for four hours of chase time. Cells were then subjected to starvation in Hanks' solution. Next, E64d and pepstatin A (dissolved in dimethyl sulfoxide) were added to the starvation medium at a final concentration

of 10 μ g/ml, and after four additional hours, the cells were treated with or without 20 μ g/ml nigericin (dissolved in ethanol) in Hanks' solution (pH 7.4). The cells were observed with confocal microscopy without fixation. Colocalization efficiency was measured using ImageJ software (<http://rsb.info.nih.gov/ij/>).

Incorporation of Cascade Blue Dextran. Cascade Blue Dextran (MW 10,000) was purchased from Molecular Probes. The reagent was added to the medium of HeLa cells to a final concentration of 0.5 mg/ml, followed by incubation at 37°C with 5% CO₂ overnight. On the next day, the cells were transferred to new medium and incubated for 4 hours chase. A plasmid expressing wild-type or the T22N mutant of Rab7 was transfected along with that encoding mRFP-LC3. The cells were observed with confocal microscopy the following day.

RESULTS

Detection of the mRFP-LC3 signal in lysosomes was dependent on autophagy. Upon induction of autophagy by starvation, autophagosomes are formed in the cytoplasm and then fuse with lysosomes. We previously reported that GFP-LC3 could be utilized for monitoring the occurrence of autophagy.¹⁵ A subset of GFP-LC3 is localized on the autophagosome membrane and, therefore, the appearance of GFP-LC3 puncta by fluorescence microscopy indicates the presence of autophagosomes. To further extend our analysis on the dynamics of autophagosome biogenesis, we constructed an mRFP marker fused to LC3 and observed its localization during autophagy. We found that the localization pattern of mRFP-LC3 was quite different from that of GFP-LC3; GFP-LC3 punctate signals were dispersed throughout the cytoplasm (Fig. 1B), whereas mRFP-LC3 punctate signals were relatively concentrated around the perinuclear region (Fig. 1A). We compared those signals to Lamp1, as a lysosome marker, because lysosomes are also generally concentrated around the perinuclear region.²⁰ We found that GFP-LC3 signals rarely colocalized with Lamp1 (Fig. 1B and C), but many of the mRFP-LC3 signals displayed Lamp1 colocalization (Fig. 1A and C).

We next investigated whether this puncta formation of mRFP-LC3 represented an artificial aggregate, a possibility reported in the case of GFP-LC3.²¹ The recruitment of LC3 to the autophagosome membrane is dependent on Atg5, another protein essential for autophagy.²² As is the case in HeLa cells (Fig. 1), mRFP-LC3 puncta displayed good colocalization with Lamp1 in wild-type mouse embryonic fibroblast cells (Fig. 2, upper panel). On the other hand, in Atg5-deficient mouse embryonic fibroblasts, mRFP-LC3 did not show punctate signals localized in lysosomes (Fig. 2A, lower panel). The C-terminal glycine of LC3 is lipidated by an ubiquitination-like system, and the substitution of the glycine residue (Gly120) to alanine abolishes the lipidation.¹⁵ This lipidated LC3, called LC3-II, binds to the autophagosome membrane and the lipid modification can be monitored due to a mobility shift by SDS-PAGE.¹⁵ mRFP-LC3-II underwent the same lipidation reaction, which is evident from the appearance of the faster migrating band following SDS-PAGE, and by the fact that this band could be detected associated with the membrane by subcellular fractionation (Fig. 2B). In sharp contrast, the mRFP-LC3 G120A mutant did not show the II form (Fig. 2B). In addition, this mutant did not show a punctate staining pattern similar to the GFP- or myc tagged LC3 G120A mutant described in a previous report (Fig. 2C).¹⁵ These results indicated that lysosomal localization of mRFP-LC3 particles was dependent on intrinsic lipidation of LC3. This criterion distinguishes the punctate signal from protein aggregates involving LC3, and indicates that mRFP-LC3 is delivered to lysosomes via a normal autophagic process.

The GFP-LC3 signal disappeared due to the lysosomal environment. The above results suggest that mRFP-LC3 is delivered to lysosomes according to the

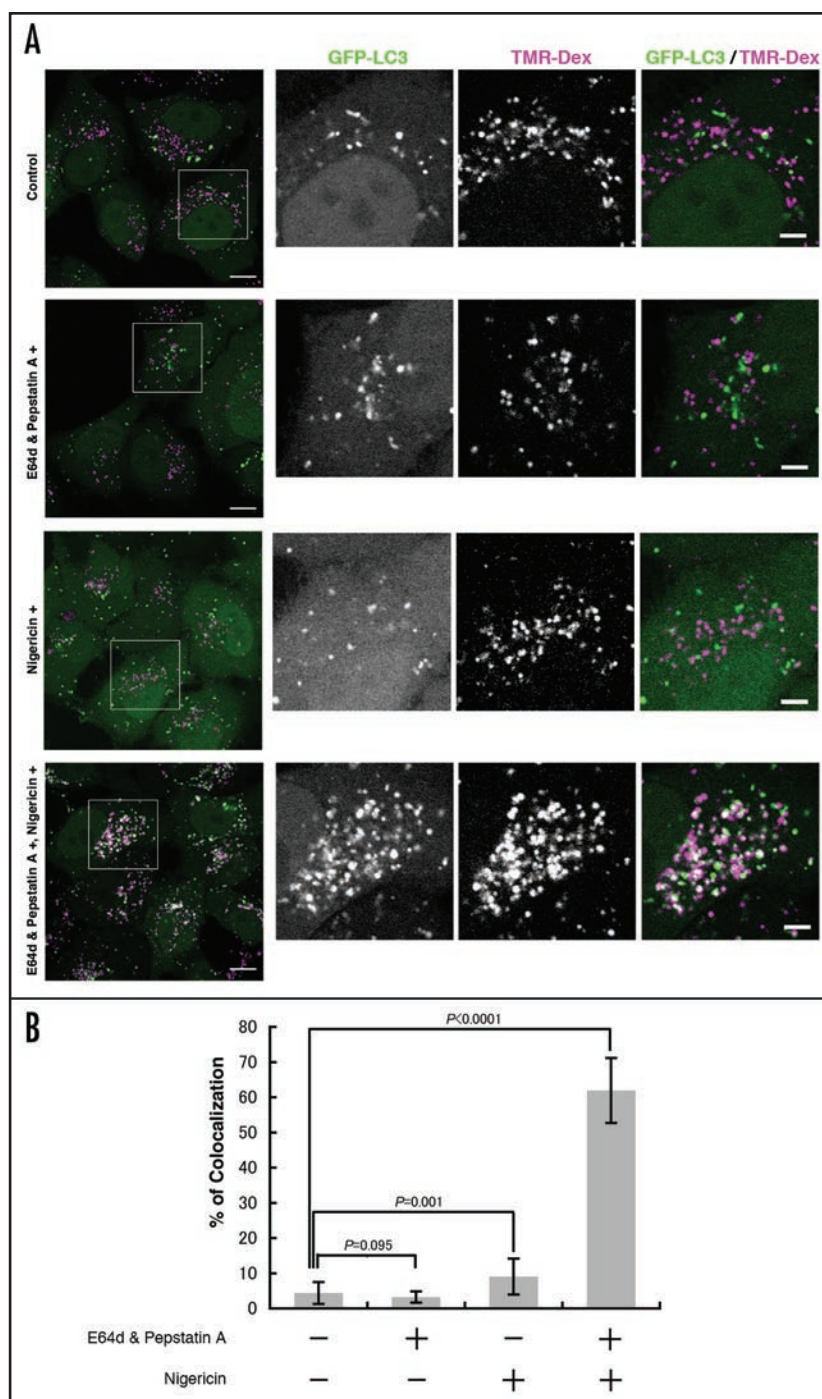


Figure 3. GFP-LC3 signals disappeared in the lysosomal environment. (A) HeLa cells stably expressing GFP-LC3 were cultured on a noncoated glass-bottom culture dish and Tetramethyl-Rhodamine (TMR) Dextran was incorporated overnight for marking lysosomes. The cells were transferred to new culture medium and incubated for 4 hours for a chase. Cells were then subjected to starvation in Hanks' solution; E64d and pepstatin A (final concentration of 10 μ g/ml) were added to the starvation medium. After 4 hours, the cells were treated with or without 20 μ g/ml nigericin for 5 min in Hanks' solution (pH 7.4). The cells were observed with confocal microscopy without fixation. The right panels are a higher magnification of the left panels. Bar indicates 10 μ m in the left panels and 2 μ m in the right panels. (B) Colocalization efficiency of GFP-LC3 puncta with TMR-Dextran was measured using ImageJ software, and shown as the percentage of total number of GFP-LC3 puncta. The value indicates average and S.D. from three independent experiments. A t-test was performed using Microsoft Excel software, and obtained p values were shown.

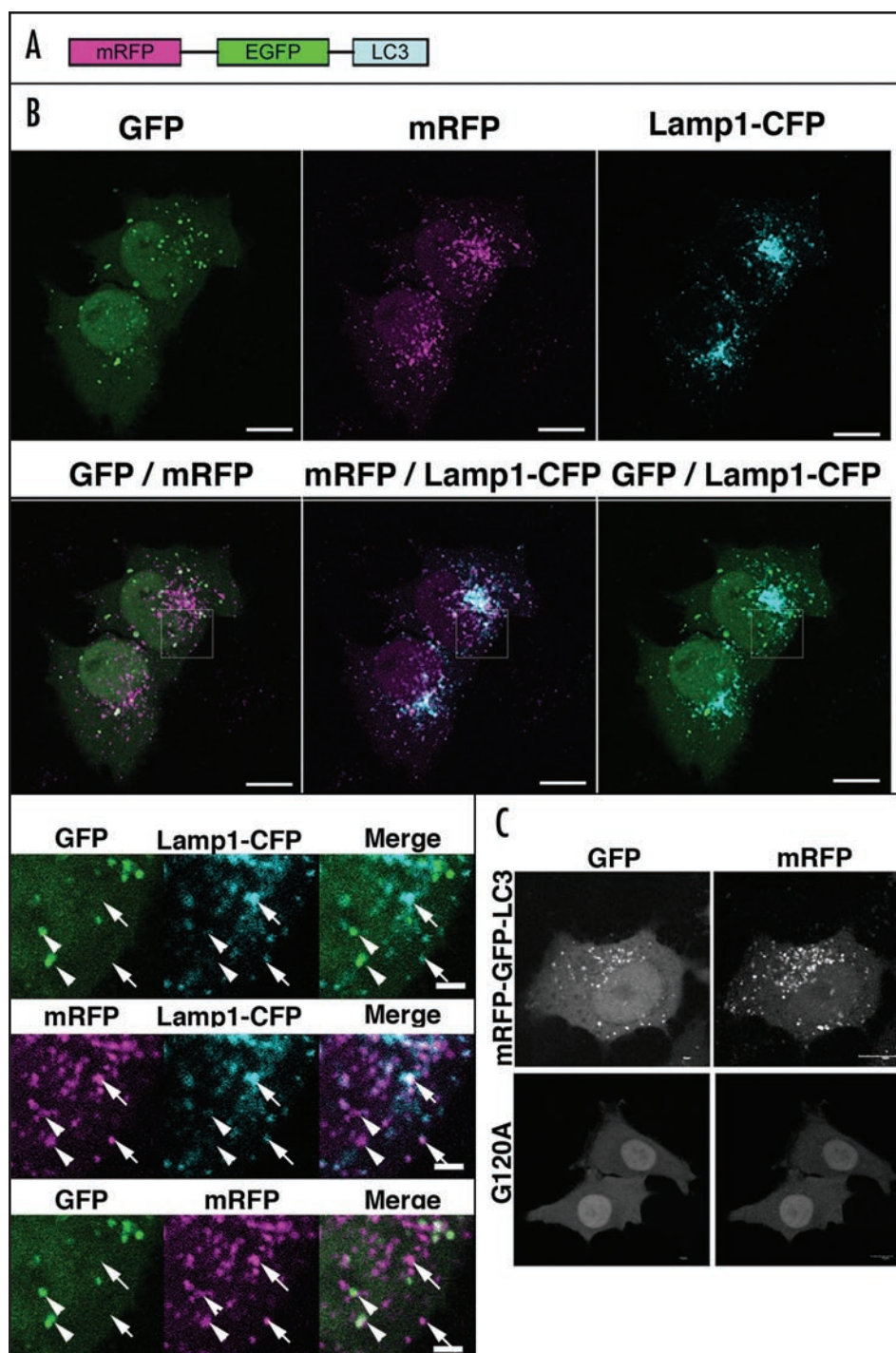


Figure 4. The GFP and mRFP signals of tflc3 show different localization patterns. (A) Diagram of tflc3 structure. (B) HeLa cells were cotransfected with plasmids expressing either tflc3 or Lamp1-CFP. Twenty-four hours after the transfection, the cells were starved in Hanks' solution for 2 hours, fixed and analyzed by microscopy. The lower panels are a higher magnification of the upper panels. Bar indicates 10 μ m in the upper panels and 2 μ m in the lower panels. Arrows in the lower panels point to typical examples of colocalized signals of mRFP and Lamp1. Arrowheads point to typical examples of colocalized particles of GFP and mRFP signals. (C) HeLa cells were transfected with plasmids encoding either tflc3 or tflc3^{G120A}. Twenty-four hours after the transfection, the cells were subjected to starvation in Hanks' solution for 2 hours, fixed and analyzed by microscopy.

intrinsic dynamics of LC3 during autophagy. We hypothesized that the GFP-LC3 signals disappear in the lysosomal environment after the fusion of autophagosomes with lysosomes, to explain why there is

localization (Fig. 3A and B). However, when nigericin was added after treatment with protease inhibitors, the efficiency of colocalization with lysosomes was significantly increased (Fig. 3A and B).

little overlap between GFP-LC3 and Lamp1. Accordingly, we tested this hypothesis by counting the number of GFP-LC3 puncta that colocalized with lysosomes marked by TMR-Dextran in cells treated with several reagents (Fig. 3). Dextran incorporation is widely used for marking lysosomes and allows observation of the organelle without fixation.^{23,24} Immunocytochemical procedures, such as fixation or permeabilization, needed for marking lysosomes using anti-Lamp1 antibody causes neutralization of the lysosomal environment. Therefore, to circumvent such a situation we used dextran incorporation without fixation for marking lysosomes.

First, we treated the cells with inhibitors for the major lysosomal proteases to investigate the involvement of lysosomal degradation. E64d is a membrane permeable inhibitor of cathepsins B, H and L,^{25,26} and pepstatin A is an inhibitor of cathepsin D and E.^{27,28} As is the case with the other lysosomal marker, Lamp1 (Fig. 1), GFP-LC3 was not colocalized with TMR-Dextran in control cells and treatment with protease inhibitors did not affect the GFP-LC3 distribution pattern (Fig. 3A and B).

Another possibility is that GFP fluorescence is attenuated by protonation of the fluorophore of the GFP molecule in lysosomal acidic conditions.²⁹ Actually, GFP has a relatively high pKa value, 6.0,²⁹ whereas, the pKa value of mRFP is 4.5.¹⁹ We therefore investigated the effect of the acidic conditions of the lysosome on fluorescence. Bafilomycin A or concanamycin A are widely used reagents to cancel lysosomal acidification by specifically inhibiting the vacuolar type ATPase.^{24,30,31} There are several reports that these drugs have effects at several steps of the autophagic process^{15,32,33} and require long incubation times (~30 min) to exert an effect.²⁴ We circumvented this situation by instead using a different reagent, nigericin. Nigericin is an ionophore that induces an exchange between K⁺ and H⁺ ions across the membrane and causes a rapid increase of the intralysosomal acidic pH, equilibrating it with that of the cytosol, which is neutral; we confirmed that five minutes incubation was sufficient for neutralization of lysosomes by staining acidic organelles using the acidotropic probe, LysoTracker (Supplemental Figure).³⁴ This rapid neutralization allowed us direct assessment of the effect of pH.

Brief treatment with nigericin after starvation had only a small effect on GFP-LC3 localization (Fig. 3A and B). However, when nigericin was added after treatment with protease inhibitors, the efficiency of colocalization with lysosomes was significantly increased (Fig. 3A and B).

This result indicates that the fluorescence from luminal GFP-LC3 was attenuated in the lysosomal acidic environment and that the protein was degraded by lysosomal hydrolases. GFP-LC3 is bound to both the outer and inner membrane of the autophagosome, and the GFP-LC3 on the outer surface is surrounded by the cytosolic environment; thus, the GFP localized on the autophagosome surface is not affected by the lysosomal environment. Taken together, these results also indicated that the GFP-LC3 initially present on the autophagosome outer surface detached from the outer membrane of the autophagosome upon, or shortly after, fusion with the lysosome; the remaining GFP-LC3 signal corresponding to the interior of the autophagosome rapidly disappeared in the lysosome lumen.

Distinction between autophagosome and autolysosome using a novel reporter protein. We noticed that this different sensitivity of GFP and mRFP to the lysosomal environment would be applicable to analyze the dynamics of autophagosomes by generating a novel marker protein, mRFP-GFP-LC3 tandem-tagged fluorescent protein (tfLC3) (Fig. 4A). If this tandem-tagged protein encountered lysosomes via an autophagic process the GFP fluorescence signals would be diminished, whereas mRFP would remain fluorescent.

Plasmids expressing tfLC3 and Lamp1-CFP were cotransfected into HeLa cells. One day after transfection, the cells were incubated in starvation conditions for 2 hours, and subjected to fixation followed by observation using confocal microscopy (Fig. 4B). As expected, the mRFP and GFP signals showed different distribution patterns (Fig. 4B). Although the GFP signals were almost completely colocalized with mRFP puncta in the cytoplasm, a substantial population of the mRFP puncta was not colocalized with GFP particles, especially around the perinuclear region (Fig. 4B and Table 1). In this region mRFP particles showed good colocalization with Lamp1 signals (Fig. 4B and Table 1). This punctate pattern was dependent on C-terminal lipidation of LC3, confirming that localization of tfLC3 was autophagy-dependent (Fig. 4C). These results are consistent with our expectation that this two-color analysis can distinguish between autophagosomes before and after the fusion with lysosomes.

We next examined the tfLC3 localization when the function of Rab7, one of the Rab family of small GTPases, is interfered with by overexpression of the T22N mutant of Rab7.^{35,36} This GDP-bound constitutive inactive mutant form exerts a dominant-negative effect over endogenous Rab7.^{35,36} HeLa cells were transfected with a plasmid encoding tfLC3 together with a plasmid expressing wild-type or T22N mutant Rab7 tagged with HA, to preselect cells for analysis based on their expression of the exogenous Rab7. The cells were fixed and then observed by confocal microscopy. In the cells expressing wild-type HA-Rab7, the signals of GFP and mRFP puncta were

Table 1 **Colocalization of mRFP and GFP signals of tfLC3 with Lamp1**

Colocalization (%)	mRFP	GFP	Lamp1
mRFP signals		24 ± 5	67 ± 12
GFP signals	86 ± 4.6		6.7 ± 2.6

Colocalization efficiency was measured by ImageJ software from images shown in Figure 4B. Values indicate average and S.D. from at least five images.

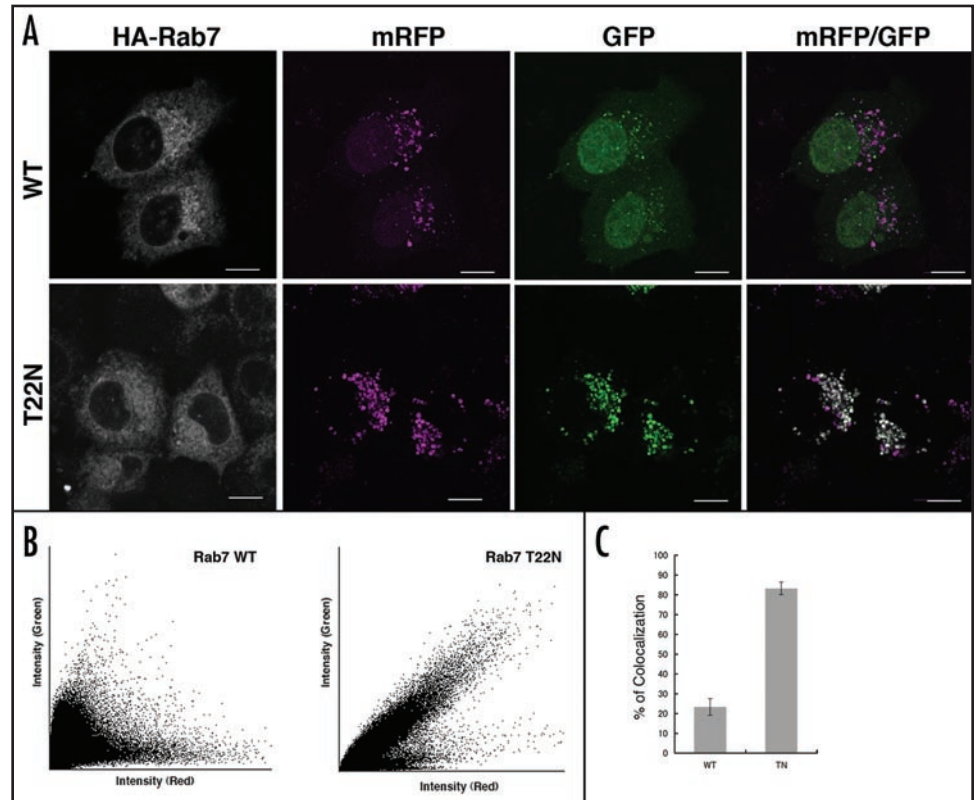


Figure 5. Overexpression of dominant negative Rab7-T22N affected mRFP-GFP-LC3 localization pattern. (A) HeLa cells were cotransfected with plasmids expressing of mRFP-GFP-LC3 and either wild-type or the T22N mutant of HA-Rab7. Twenty-four hours after transfection, the cells were subjected to starvation in Hanks' solution for 2 hours, fixed and subjected to immunocytochemistry using anti-HA antibody. Anti-mouse antibody conjugated with Alexa488 was used as second antibody. Bar indicates 10 μ m. (B) Each correlation plot is derived from a field of view shown in (A). (C) Colocalization efficiency of mRFP with GFP signals of tfLC3 puncta was measured using ImageJ software, and shown as the percentage of the total number of mRFP puncta. The value indicates average and S.D. from at least five images.

not entirely colocalized, as is the case of the cells without Rab7 transfection (Figs. 5, A, B and C). However, in the cells expressing the HA-Rab7 T22N mutant, signals of tfLC3 puncta accumulated around the perinuclear region, and the GFP and mRFP signals almost completely overlapped (Figs. 5A–C). This result is consistent with previous reports showing that expression of the GDP-form of Rab7, the T22N mutant, or RNAi-mediated knockdown of Rab7 affect the maturation process, but not the formation, of autophagosomes.^{11,12}

Rab7 is an essential protein for endosome and lysosome biogenesis, including their acquisition of luminal acidity and degradative activity.^{35,36} Thus, there is a possibility that the dominant-negative effect of Rab7 T22N on tfLC3 was not due to prevention of the fusion of autophagosomes and lysosomes, but rather was due to inhibition

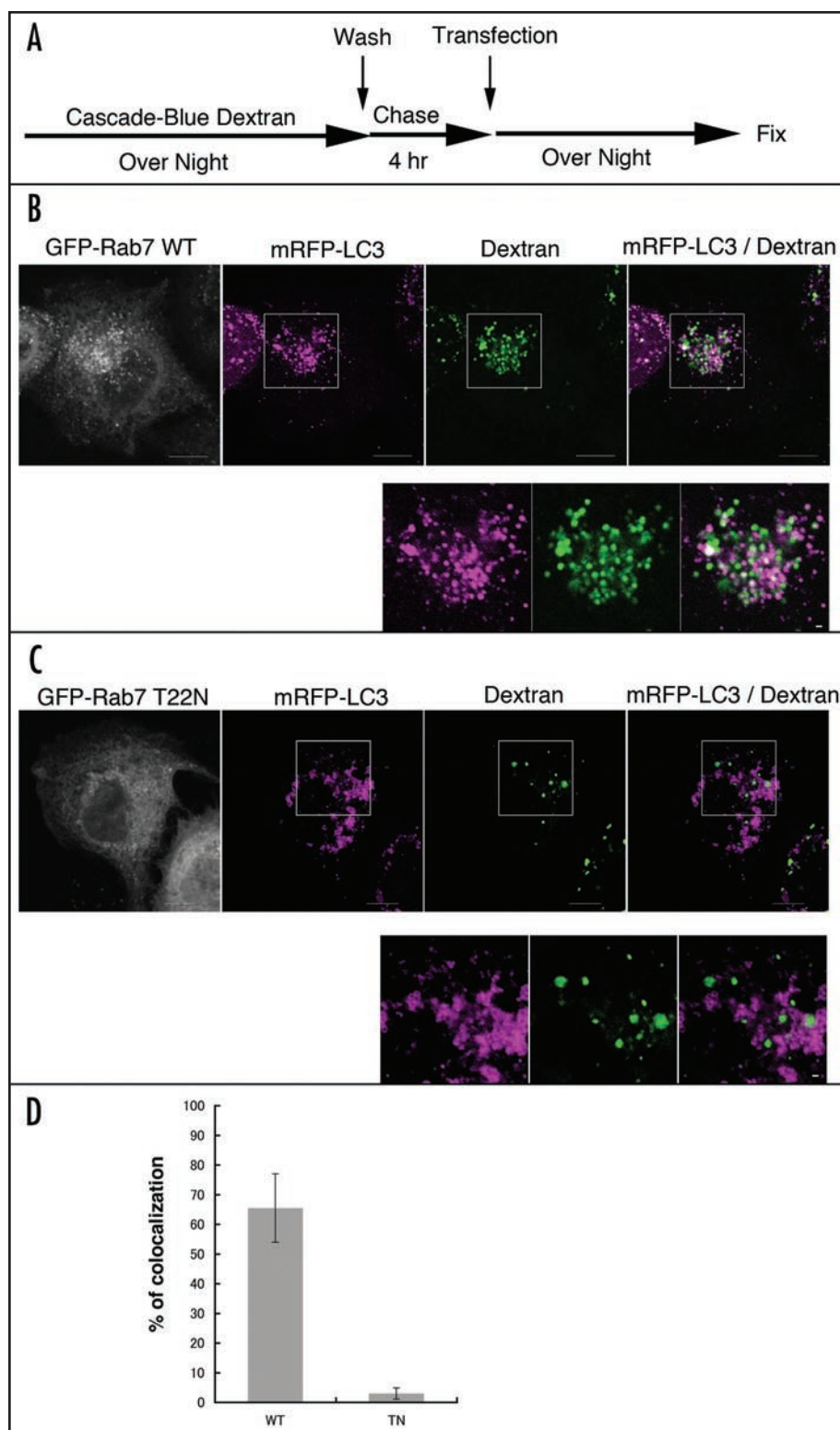


Figure 6. Overexpression of Rab7 T22N prevented the delivery of mRFP-LC3 to lysosomes. (A) The scheme of incorporation and transfection experiments is shown. HeLa cells preloaded with Cascade-Blue Dextran for marking lysosomes were cotransfected with plasmids expressing mRFP-LC3 and either the wild-type (B) or T22N mutant (C) of GFP-Rab7 as shown in (A). Twenty-four hours after the transfection, the cells were starved in Hanks' solution for 2 hours, fixed and analyzed by microscopy. The lower panels are a higher magnification of the upper panels. Bar indicates 10 μ m in the upper panels and 1 μ m in the lower panels. (D) Colocalization efficiency of mRFP-LC3 with Cascade-Blue Dextran signals was measured using ImageJ software, and shown as the percentage of the total number of mRFP puncta. The value indicates average and S.D. from at least five images.

of lysosomal biogenesis. To negate this possibility, we designed an experiment to detect the fusion between autophagosomes and lysosomes. HeLa cells that had incorporated Cascade-Blue Dextran via endocytosis (for marking lysosomes) were cotransfected with plasmids expressing mRFP-LC3 and either GFP-Rab7 wild-type or the T22N mutant (Fig. 6A). In this case, we used the GFP tag to preselect Rab7-expressing cells for observation without permeabilization of cells that would cause loss of the incorporated Dextran. In the cells expressing GFP-Rab7 wild-type, the signals of mRFP-LC3 particles displayed good colocalization with lysosomes marked by preincorporated dextran (Fig. 6B and D). On the other hand, in the cells expressing the GFP-Rab7 T22N mutant, mRFP-LC3 signals accumulated around the perinuclear region and did not colocalize with Cascade-Blue Dextran (Fig. 6C and D). This result confirmed that Rab7 T22N expression inhibited fusion between autophagosomes and lysosomes.

DISCUSSION

In this study we found that GFP-LC3 signals disappeared within the lysosomal environment, whereas mRFP-LC3 signals persisted. Moreover, a substantial population of mRFP-GFP-LC3, named tLC3, which colocalized with a lysosomal marker, exhibited only the RFP signal.

These results indicate two important facts. First, the disappearance of the GFP signal in autolysosomes must be a quite rapid event; if the disappearance was gradual, there should be some overlap of the lysosomal marker and the remnant of the GFP signal. Our present study shows that both attenuation of fluorescence and subsequent degradation of GFP-LC3 in lysosomal conditions causes disappearance of GFP-LC3 signals in autolysosomes. In the case of yeast, GFP-Atg8 signals can be observed in the vacuole, which is analogous to the lysosome;³⁷ however, the pKa value of GFP is 6.0²⁹ and the pH of the yeast vacuole is approximately 6.2,³⁸ much higher than the 4.8 of mammalian lysosomes.^{24,34} On the other hand, mRFP is not attenuated in lysosomal conditions due to its lower pKa value, and is probably resistant to lysosomal degradation. Attenuation of fluorescence is caused by protonation of its fluorophore and could occur within <1 ms, whereas protein conformational changes or degradation could occur over millisecond and longer time frames.²⁹ Therefore, we can monitor the maturation process only for a short time after fusion takes place.

Second, our result provides novel information about the dynamics of LC3. The carboxyl terminus of LC3 is modified with phosphatidylethanolamine by an ubiquitination-like system, and the lipidated protein is bound to isolation

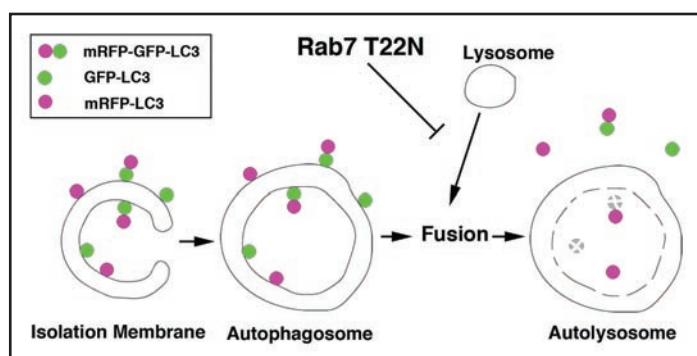


Figure 7. Schematic diagram of the maturation steps of autophagosome biogenesis. Under starvation condition, a cup shaped isolation membrane is formed and engulfs a portion of the cytoplasm. The isolation membrane finally becomes enclosed, forming a double-membrane autophagosome. Subsequently, autophagosomes fuse with lysosomes in a Rab7-dependent manner, to become autolysosomes. During this process LC3 is lipidated at its C terminus and recruited to both the inner and outer membrane of the autophagosome. After or before fusion with lysosomes, LC3 bound to the outer membrane is probably delipidated and detached from the outer membrane of the autolysosomes. The signals from GFP that was present within the inner autophagosome membrane disappear in the lysosomal environment, but mRFP signals are relatively stable. Thus, GFP-LC3 can be used as a marker for the isolation membrane and autophagosome membrane but not the autolysosome, whereas mRFP-LC3 can be used as a marker for all three compartments. That is, tflc3 bound on the isolation membrane and autophagosome shows both GFP and mRFP fluorescence; after fusion with lysosomes, the GFP signals are diminished, and only mRFP signals can be detected.

membranes (Fig. 7). Eventually both sides of the autophagosomal double-layered membrane are supposed to be decorated by lipidated LC3. In the case of yeast, Atg8, the orthologue of LC3, is finally deconjugated by the action of the Atg4 cysteine protease;³⁹ however, in the case of mammal, little is known regarding the delipidation process. Our results indicate that autolysosomes are devoid of LC3 bound to the outer membrane, because LC3 on the outer autophagosome surface is surrounded by the cytosolic (i.e., not the lysosomal) environment and should continue to fluoresce. Therefore, our observations suggest that LC3 on the outer surface is liberated from the membrane at some stage of autophagosome maturation, or even before completion, although we cannot rule out the possibility of rapid cleavage from the lysosome surface immediately following fusion (Fig. 7). As is the case in yeast, the delipidation of LC3 is supposed to be involved in this detachment and caused by a second Atg4-dependent cleavage.³⁹ The mechanistic significance of this delipidation is an interesting issue and the assay using tflc3 will provide a useful method for the analysis.

Rab7 is involved in regulation of late endosomal membrane traffic and lysosome biogenesis,^{35,36} and it is also necessary for autophagosome maturation.^{11,12} We showed that overexpression of the Rab7 T22N mutant caused accumulation of tflc3 puncta exhibiting both GFP and mRFP fluorescence. mRFP-LC3 was not colocalized with lysosomes in the cells overexpressing the Rab7 T22N mutant. Using quantitative electron microscopy, Jager et al. showed that late autophagosomes containing intact cytosol were accumulated by knockdown of Rab7, and concluded that Rab7 is involved in the final maturation step of autophagosome.¹² However, their results could not exclude the possibility that knockdown of Rab7 led to lysosome dysfunction, such as inhibition of transport of hydrolases to lysosomes or acidification of the lysosome lumen, and that defects in the degradation of late autophagosomes is due to such lysosome

dysfunction. Gutierrez et al. also reported the involvement of Rab7 in the autophagic process.¹¹ They showed that monodansylcadaverine (MDC) is not colocalized with a lysosomal marker, which is dextran incorporated via fluid phase endocytosis. However, MDC also stains other acidic organelles, meaning that it also stains late endosomes and lysosomes.⁴⁰ In addition, Gutierrez et al. used dextran as a lysosome marker in the cells stably expressing the Rab7 T22N mutant. It is highly possible that overexpression of the Rab7 T22N mutant inhibits the endocytic pathway and prevents transport of dextran to MDC-labeled late endosomes or lysosomes. This time, we circumvented these problems by preloading the TMR-dextran dye into lysosomes before transfection with the Rab7 T22N mutant, and we used fluorescent protein fused-LC3 as a specific autolysosome marker to overcome the nonspecific aspects of MDC. Although the conclusion we obtained is the same as in the previous two reports, we think that our analysis provides the first definitive proof for the role of Rab7 in autophagosome-lysosome fusion.

The yeast vacuole is much larger than the lysosome; once autophagosome-vacuole fusion takes place, the inner autophagosome membrane appears as an autophagic body in the large vacuole lumen. However, in the case of mammalian cells, a single fusion event is not so evident just with an ultrastructural analysis. The dual color analysis using tflc3 presented in this study enables a direct and rapid assessment as to whether fusion takes place with a relatively simple method compared to electron microscopy analysis. We believe that this method will allow us to gain further insight into the molecular mechanisms that regulate the maturation and the fusion step of the autophagic pathway in mammalian cells.

Acknowledgements

We are grateful to Dr. Kyoshei Umebayashi (Osaka University, Japan) for the Rab7 plasmids, Dr. Roger Y. Tsien (University of California, San Diego, USA) for the gift of mRFP1 cDNA, Dr. Noboru Mizushima (Tokyo Medical and Dental University, Japan) for the gift of Atg5^{-/-} MEF cells, and Dr. Daniel Klionsky (University of Michigan, Michigan, USA) for editing manuscript. This work was supported in part by Special Coordination Funds for Promoting Science and Technology of the Ministry of Education, Culture, Sports, Science, and Technology (MEXT).

References

- Seglen PO, Bohley P. Autophagy and other vacuolar protein degradation mechanisms. *Experientia* 1992; 48:158-72.
- Yoshimori T. Autophagy: A regulated bulk degradation process inside cells. *Biochem Biophys Res Commun* 2004; 313:453-8.
- Komatsu M, Waguri S, Chiba T, Murata S, Iwata J, Tanida I, Ueno T, Koike M, Uchiyama Y, Kominami E, Tanaka K. Loss of autophagy in the central nervous system causes neurodegeneration in mice. *Nature* 2006; 441:880-4.
- Hara T, Nakamura K, Matsui M, Yamamoto A, Nakahara Y, Suzuki-Migishima R, Yokoyama M, Mishima K, Saito I, Okano H, Mizushima N. Suppression of basal autophagy in neural cells causes neurodegenerative disease in mice. *Nature* 2006; 441:885-9.
- Nakagawa I, Amano A, Mizushima N, Yamamoto A, Yamaguchi H, Kamimoto T, Nara A, Funao J, Nakata M, Tsuda K, Hamada S, Yoshimori T. Autophagy defends cells against invading group A *Streptococcus*. *Science* 2004; 306:1037-40.
- Ogawa M, Yoshimori T, Suzuki T, Sagara H, Mizushima N, Sasakawa C. Escape of intracellular *Shigella* from autophagy. *Science* 2005; 307:727-31.
- Ravikumar B, Duden R, Rubinstein DC. Aggregate-prone proteins with polyglutamine and polyalanine expansions are degraded by autophagy. *Hum Mol Genet* 2002; 11:1107-17.
- Kamimoto T, Shoji S, Hidvegi T, Mizushima N, Umebayashi K, Perlmutter DH, Yoshimori T. Intracellular inclusions containing mutant α_1 -antitrypsin Z are propagated in the absence of autophagic activity. *J Biol Chem* 2005; 281:4467-76.
- Eskelinen E-L. Maturation of autophagic vacuoles in mammalian cells. *Autophagy* 2005; 1:1-10.
- Nara A, Mizushima N, Yamamoto A, Kabeya Y, Ohsumi Y, Yoshimori T. SKD1 AAA ATPase-dependent endosomal transport is involved in autolysosome formation. *Cell Struct Funct* 2002; 27:29-37.
- Gutierrez MG, Munafò DB, Beron W, Colombo MI. Rab7 is required for the normal progression of the autophagic pathway in mammalian cells. *J Cell Sci* 2004; 117:2687-97.

12. Jager S, Bucci C, Tanida I, Ueno T, Kominami E, Saftig P, Eskelinen EL. Role for Rab7 in maturation of late autophagic vacuoles. *J Cell Sci* 2004; 117:4837-48.
13. Atlashkin V, Kreykenbohm V, Eskelinen EL, Wenzel D, Fayyazi A, Fischer von Mollard G. Deletion of the SNARE *vti1b* in mice results in the loss of a single SNARE partner, syntaxin 8. *Mol Cell Biol* 2003; 23:5198-207.
14. Esselens C, Oorschot V, Baert V, Raemaekers T, Spittaels K, Serneels L, Zheng H, Saftig P, De Strooper B, Klumperman J, Annaert W. Presenilin 1 mediates the turnover of telencephalin in hippocampal neurons via an autophagic degradative pathway. *J Cell Biol* 2004; 166:1041-54.
15. Kabeya Y, Mizushima N, Ueno T, Yamamoto A, Kirisako T, Noda T, Kominami E, Ohsumi Y, Yoshimori T. LC3, a mammalian homologue of yeast Apg8p, is localized in autophagosome membranes after processing. *EMBO J* 2000; 19:5720-8.
16. Tanida I, Ueno T, Kominami E. LC3 conjugation system in mammalian autophagy. *Int J Biochem Cell Biol* 2004; 36:2503-18.
17. Mizushima N. Methods for monitoring autophagy. *Int J Biochem Cell Biol* 2004; 36:2491-502.
18. Kuma A, Hatano M, Matsui M, Yamamoto A, Nakaya H, Yoshimori T, Ohsumi Y, Tokuhiya T, Mizushima N. The role of autophagy during the early neonatal starvation period. *Nature* 2004; 432:1032-6.
19. Campbell RE, Tour O, Palmer AE, Steinbach PA, Baird GS, Zacharias DA, Tsien RY. A monomeric red fluorescent protein. *Proc Natl Acad Sci USA* 2002; 99:7877-82.
20. Matteoni R, Kreis TE. Translocation and clustering of endosomes and lysosomes depends on microtubules. *J Cell Biol* 1987; 105:1253-65.
21. Kuma A, Matsui M, Mizushima N. LC3, an autophagosome marker, can be incorporated into protein aggregates independent of autophagy: Caution in the interpretation of LC3 localization. *Autophagy* 2007; 3:323-8.
22. Mizushima N, Yamamoto A, Hatano M, Kobayashi Y, Kabeya Y, Suzuki K, Tokuhiya T, Ohsumi Y, Yoshimori T. Dissection of autophagosome formation using *Apg5*-deficient mouse embryonic stem cells. *J Cell Biol* 2001; 152:657-68.
23. Bright NA, Gratian MJ, Luzio JP. Endocytic delivery to lysosomes mediated by concurrent fusion and kissing events in living cells. *Curr Biol* 2005; 15:360-5.
24. Yoshimori T, Yamamoto A, Moriyama Y, Futai M, Tashiro Y. Bafilomycin A1, a specific inhibitor of vacuolar-type H⁺-ATPase, inhibits acidification and protein degradation in lysosomes of cultured cells. *J Biol Chem* 1991; 266:17707-12.
25. Tamai M, Matsumoto K, Omura S, Koyama I, Ozawa Y, Hanada K. In vitro and in vivo inhibition of cysteine proteinases by EST, a new analog of E-64. *J Pharmacobiodyn* 1986; 9:672-7.
26. Tamai M, Yokoo C, Murata M, Oguma K, Sota K, Sato E, Kanaoka Y. Efficient synthetic method for ethyl (+)-(2S,3S)-3-[(S)-3-methyl-1-(3-methylbutylcarbamoyl)butylcarbamoyl]-2-oxiranecarboxylate (EST), a new inhibitor of cysteine proteinases. *Chem Pharm Bull (Tokyo)* 1987; 35:1098-104.
27. Umezawa H, Aoyagi T, Morishima H, Matsuzaki M, Hamada M. Pepstatin, a new pepsin inhibitor produced by Actinomycetes. *J Antibiot (Tokyo)* 1970; 23:259-62.
28. Aoyagi T, Morishima H, Nishizawa R, Kunimoto S, Takeuchi T. Biological activity of pepstatins, pepstanone A and partial peptides on pepsin, cathepsin D and renin. *J Antibiot (Tokyo)* 1972; 25:689-94.
29. Kneen M, Farinas J, Li Y, Verkman AS. Green fluorescent protein as a noninvasive intracellular pH indicator. *Biophys J* 1998; 74:1591-9.
30. Woo JT, Shinohara C, Sakai K, Hasumi K, Endo A. Inhibition of the acidification of endosomes and lysosomes by the antibiotic concanamycin B in macrophage J774. *Eur J Biochem* 1992; 207:383-9.
31. Woo JT, Shinohara C, Sakai K, Hasumi K, Endo A. Isolation, characterization and biological activities of concanamycins as inhibitors of lysosomal acidification. *J Antibiot (Tokyo)* 1992; 45:1108-16.
32. Yamamoto A, Tagawa Y, Yoshimori T, Moriyama Y, Masaki R, Tashiro Y. Bafilomycin A1 prevents maturation of autophagic vacuoles by inhibiting fusion between autophagosomes and lysosomes in rat hepatoma cell line, H-4-II-E cells. *Cell Struct Funct* 1998; 23:33-42.
33. Mousavi SA, Kjekshus R, Berg TO, Seglen PO, Berg T, Brech A. Effects of inhibitors of the vacuolar proton pump on hepatic heterophagy and autophagy. *Biochim Biophys Acta* 2001; 1510:243-57.
34. Ohkuma S, Poole B. Fluorescence probe measurement of the intralysosomal pH in living cells and the perturbation of pH by various agents. *Proc Natl Acad Sci USA* 1978; 75:3327-31.
35. Bucci C, Thomsen P, Nicoziani P, McCarthy J, van Deurs B. Rab7: A key to lysosome biogenesis. *Mol Biol Cell* 2000; 11:467-80.
36. Feng Y, Press B, Wandinger-Ness A. Rab 7: An important regulator of late endocytic membrane traffic. *J Cell Biol* 1995; 131:1435-52.
37. Suzuki K, Kamada Y, Ohsumi Y. Studies of cargo delivery to the vacuole mediated by autophagosomes in *Saccharomyces cerevisiae*. *Dev Cell* 2002; 3:815-24.
38. Preston RA, Murphy RF, Jones EW. Assay of vacuolar pH in yeast and identification of acidification-defective mutants. *Proc Natl Acad Sci USA* 1989; 86:7027-31.
39. Kirisako T, Ichimura Y, Okada H, Kabeya Y, Mizushima N, Yoshimori T, Ohsumi M, Takao T, Noda T, Ohsumi Y. The reversible modification regulates the membrane-binding state of Apg8/Aut7 essential for autophagy and the cytoplasm to vacuole targeting pathway. *J Cell Biol* 2000; 151:263-76.
40. Bampton ET, Goemans CG, Niranjana D, Mizushima N, Tolkovsky AM. The dynamics of autophagy visualized in live cells: From autophagosome formation to fusion with endo/lysosomes. *Autophagy* 2005; 1:23-36.